Nitin K. Garg
Nonlinear Dynamics Lab,
Department of Mechanical & Aerospace Engineering, University of Florida,
Gainesville, FL 32611
e-mail: nitingar@ufl.edu

Brian P. Mann[1]
Dynamical Systems Lab,
Department of Mechanical & Aerospace Engineering, University of Missouri,
Columbia, MO 65211
e-mail: mannbr@missouri.edu

Nam H. Kim
Structural and Multi-disciplinary Optimization Lab, Department of Mechanical & Aerospace Engineering, University of Florida,
Gainesville, FL 32611
e-mail: nkim@ufl.edu

Mohammad H. Kurdi
Machine Tool Research Center,
Department of Mechanical & Aerospace Engineering, University of Florida,
Gainesville, FL 32611
e-mail: mhkurdi@ufl.edu

Stability of a Time-Delayed System With Parametric Excitation

This paper investigates two different temporal finite element techniques, a multiple element (h-version) and single element (p-version) method, to analyze the stability of a system with a time-periodic coefficient and a time delay. The representative problem, known as the delayed damped Mathieu equation, is chosen to illustrate the combined effect of a time delay and parametric excitation on stability. A discrete linear map is obtained by approximating the exact solution with a series expansion of orthogonal polynomials constrained at intermittent nodes. Characteristic multipliers of the map are used to determine the unstable parameter domains. Additionally, the described analysis provides a new approach to extract the Floquet transition matrix of time periodic systems without a delay. [DOI: 10.1115/1.2432357]

Keywords: bifurcation, delay differential equations, parametric excitation, Mathieu equation

1 Introduction

The stability of systems governed by time-periodic differential equations is important to various fields of science and engineering. For instance, recent literature has described applications in high-speed milling [1–5], quantum mechanics, structures under oscillating loads, and rotating helicopter blades [6].

Some of the methods available for stability analysis are Hill's method [7–9], Floquet theory [10–16], and perturbation [7,17,18]. Sinha and Wu [19], Sinha [20], Sinha et al. [21–23], Butcher et al. [24], Ma et al. [25,26], Bueler et al. [27], and Szabo and Butcher [28] have used Chebyshev polynomials to analyze the stability and control of time-periodic systems. The effect of time delay on control stability has been examined by Yang and Wu [6], Horng and Chou [29], and Chung and Sun [30], who studied the effect of a time delay on structural dynamics.

The delayed damped Mathieu equation (DDME) provides a representative system with both a time delay and parametric excitation. Mathieu [31] used this equation, without the time-delay and damping terms, to study the oscillations of an elliptic membrane. Bellman and Cooke [32] and Bhatt and Hsu [33] both made attempts to lay out the criteria for stability using the D-subdivision [34] method combined with the theorem of Pontryagin [35]. Insperger and Stépán have used an analytical and semi-discretization approach, which is applicable to a combination of problems with finite and functional time delays, to examine the stability of the DDME [36–38].

The use of orthogonal polynomials to solve systems with parametric excitation and no time delay has been adopted by many authors. For instance, Chang et al. [39] studied the response of linear dynamic systems. Sinha and Chou [40] and Sinha et al. [13] used orthogonal polynomials to investigate the behavior of time-periodic differential equations. Orthogonal polynomials are used because they decouple the successive solutions, as presented in Ref. [41], which will increase the rate of convergence, thereby making the process less computationally expensive. In this paper, interpolated orthogonal polynomials are used to determine the stability of a system with both parametric excitation and time delayed feedback.

The present work describes two different temporal finite element analysis approaches that can be used to ascertain the stability behavior of both linear autonomous and nonautonomous systems with a single time delay (see previous work in Refs. [4] and [42–46]). In particular, this paper examines the stability of the DDME using temporal finite element analysis. A set of orthogonal polynomials, constrained for C^1 continuity, are used to obtain a discrete linear map that closely approximates the exact solution. Characteristic multipliers of the map, which are obtained from the finite-dimensional monodromy operator that closely approximates the actual infinite-dimensional system, are then used to determine the stable and unstable parameter domains.

Two different approaches are used to formulate dynamic maps that describe the system evolution: (i) a multiple element method is described that divides the minimum time period of the system into a finite number of temporal elements. An approximate solution is then obtained for a single period as a linear combination of interpolated polynomials. This technique employs cubic polynomials as trial functions to approximate the exact solution. Asymptotic convergence of the approximated solution to the exact solution is obtained by increasing the number of elements that discretize the time domain. This approach is called *h-convergence* as in spatial finite element analysis. (ii) A single-element method that utilizes a linear combination of higher-order orthogonal polynomials, coupled with C^1 continuity, is applied in the second approach. These polynomials approximate the exact solution by utilizing a single temporal element. Asymptotic convergence of the approximated solution to the exact solution is obtained by increas-

[1]Corresponding author.

Contributed by the Dynamic Systems, Measurement, and Control Division of ASME for publication in the JOURNAL OF DYNAMIC SYSTEMS MEASUREMENT, AND CONTROL. Manuscript received September 10, 2004; final manuscript received May 11, 2006. Assoc. Editor: Jordan Berg.

ing the polynomial order. This methodology, where solution convergence is obtained by increasing the polynomial order while keeping the number of elements fixed, is known as *p-convergence*.

2 Delayed Mathieu Equation

The delayed damped Mathieu equation can be written as

$$\ddot{x}(t) + \kappa\dot{x}(t) + [\delta + \epsilon\cos(\omega t)]x(t) = bx(t-\tau) \tag{1}$$

where Eq. (1) has a period of $T=2\pi/\omega$, a damping coefficient of κ, a time delay of $\tau=2\pi$, a constant and time periodic coefficient $\delta+\epsilon\cos(\omega t)$, and a gain term, b, which scales the influence of the delayed feedback state.

Before looking at the stability of delayed damped Mathieu equation (DDME), it is imperative to consider the various types of bifurcations that may occur in parameter space. Section 3 provides an overview of several types of bifurcations that are of potential interest for the system under study.

3 Bifurcations

This section provides an overview of Floquet theory for time periodic systems prior to discussing the additional considerations for time periodic systems with a time delay. In general, a linear periodic ordinary differential equation can be written as

$$\dot{\vec{X}}(t) = \mathbf{A}(t)\vec{X}(t) \tag{2}$$

where $\vec{X}(t)$ is an n-dimensional state vector, and the matrix $\mathbf{A}(t)$ is a time-periodic coefficient with a period T. Equation (2) has a fundamental set of n-linearly independent solutions, x_i, where $i=1,2,\ldots,n$. This implies that the states one period into the future, $x_i(t+T)$, must be a linear combination of states at the current time $x_i(t)$. This relationship can be written as

$$\vec{X}(t+T) = \varphi(T)\vec{X}(t) \tag{3}$$

where $\varphi(T)$ is a $n\times n$ Floquet transition matrix [47]. Eigenvalues of the Floquet transition matrix $(\mu_m, m=1,2,\ldots,n)$, also known as characteristic multipliers, are unique for a given system and can be calculated from

$$\det[\mu I - \varphi(T)] = 0 \tag{4}$$

The form of the mth characteristic multiplier is $\mu_m=e^{\lambda_m T}$, which relates the asymptotic stability behavior in the discrete time domain to the asymptotic stability behavior in the continuous time domain with the characteristic exponent λ_m. The system is asymptotically stable if all characteristic multipliers (μ_m) are in a modulus of less than unity. Depending on the manner in which the characteristic multiplier μ leaves the unit circle, one can characterize the loss of stability from three distinct routes:

1. A characteristic multiplier penetrates the unit circle through +1 (real axis), resulting in one of the following three bifurcations: *transcritical, symmetry-breaking, and cyclic fold bifurcations*.
2. A characteristic multiplier leaves the unit circle through −1 (real axis), resulting in a *period-doubling* bifurcation.
3. A pair of complex conjugate characteristic multipliers exits the unit circle away from real axis, resulting in a secondary *Hopf* or *Neimark-Sacker* bifurcation.

The stability analysis of a time-periodic system is closely related to the same system with an introduction of a time delay. For instance, consider the following delay oscillator:

$$\dot{\vec{X}}(t) = \mathbf{A}(t)\vec{X}(t-\tau) \tag{5}$$

where τ is the delay. As in the time-periodic case, the form of the solution can be written as $\vec{X}=\vec{p}(t)e^{\lambda t}$. However, a primary difference exists between the monodromy operator of Eq. (5) and the Floquet transition matrix of Eq. (2). For instance, Ref. [48] notes that the time periodic system will have a finite-dimensional Floquet transition matrix, but the delay oscillator system will have an infinite-dimensional monodromy operator. Also, in contrast to the classical time-periodic case, the time-delayed system will have an infinite number of characteristic multipliers. The resulting criteria for asymptotic stability now requires the infinite number of characteristic multipliers to have a modulus of <1; this criteria is analogous to requiring the infinite number of characteristic exponents to be negative and real.

The infinite-dimensional monodromy operator is problematic from the analyst point of view since it prohibits a closed-formed solution. In spite of this problem, one can approach this problem from a practical standpoint, by constructing a finite-dimensional monodromy operator that closely approximates the stability characteristics of the infinite-dimensional monodromy operator. This is the underlying approach followed throughout this paper. Although the presented approach can still be used to produce a monodromy operator matrix of higher and higher dimensions, it is surmised that this is an unnecessary task since the asymptotic stability behavior is observed to be accurately captured by relatively smaller-dimensional matrix representations of the infinite-dimensional monodromy operator.

4 Multiple Element Dynamic Map (*h-Version*)

Systems governed by time-delay differential equations do not have a closed-form solution [49,50]. In order to predict their behavior, an approximation to exact solution is required. Temporal finite element analysis (TFEA) is a technique to examine the dynamic behavior of a system with a single time delay, such as the delayed damped Mathieu equation. After formulating a finite-dimensional dynamic map, which is an approximation to the infinite-dimensional monodromy matrix, the characteristic multipliers of the map are used to determine the system stability.

The stability behavior of Eq. (1) is investigated by dividing a period of the system $T=2\pi/\omega$ into a finite number of elements. The approximate solution, within the jth element, can then be written as

$$x_j(t) \approx \sum_{i=1}^{4} a_{ji}^{n}\phi_i[\sigma_j(t)] \tag{6}$$

where $\phi_i[\sigma_j(t)]$ are the cubic Hermite polynomials, or trial functions defined in Eq. (7) and $\sigma_j(t)$ is the local time within the jth element of the nth period. A specific benefit of the chosen trial functions is their end conditions; this allows one to match the velocity and displacement at interelement nodes and reduce the number of coefficients required in the multiple element monodromy operator of Sec. 4.1. The trial function expressions are

$$\phi_1(\sigma_j) = 1 - 3\left(\frac{\sigma_j}{t_j}\right)^2 + 2\left(\frac{\sigma_j}{t_j}\right)^3 \tag{7a}$$

$$\phi_2(\sigma_j) = t_j\left[\left(\frac{\sigma_j}{t_j}\right) - 2\left(\frac{\sigma_j}{t_j}\right)^2 + \left(\frac{\sigma_j}{t_j}\right)^3\right] \tag{7b}$$

$$\phi_3(\sigma_j) = 3\left(\frac{\sigma_j}{t_j}\right)^2 - 2\left(\frac{\sigma_j}{t_j}\right)^3 \tag{7c}$$

$$\phi_4(\sigma_j) = t_j\left[-\left(\frac{\sigma_j}{t_j}\right)^2 + \left(\frac{\sigma_j}{t_j}\right)^3\right] \tag{7d}$$

The time for each element is $t_j=T/E$, and E is the number of elements into which the period T is divided. Substitution of the approximate solution into Eq. (1) gives an error $e_{rr}(t)$

$$\sum_{i=1}^{4} a_{ji}^{n}\ddot{\phi}_i[\sigma_j(t)] + \kappa\sum_{i=1}^{4} a_{ji}^{n}\dot{\phi}_i[\sigma_j(t)] + [\delta + \epsilon\cos(\omega t)]\sum_{i=1}^{4} a_{ji}^{n}\phi_i[\sigma_j(t)] - b\sum_{i=1}^{4} a_{ji}^{n-1}\phi_i[\sigma_j(t)] = e_{rr}(t) \tag{8}$$

where a_{ji}^{n-1} represents the coefficients of the assumed solution from the previous period.

The next step requires weighting the approximation error and setting the result of the residual error to zero. This gives two equations per element to solve for the coefficients (a_{ji}). The purpose of weighting the residual error (e_{rr}) is to select from an infinite number of possible solutions ($-\infty < a_{ij} < +\infty$), a best solution as close as possible to the exact solution. The resulting residual error is

$$\int_0^{t_j}\left\{\sum_{i=1}^{4} a_{ji}^{n}\ddot{\phi}_i[\sigma_j(t)]\psi_p[\sigma_j(t)] + \kappa\sum_{i=1}^{4} a_{ji}^{n}\dot{\phi}_i[\sigma_j(t)]\psi_p[\sigma_j(t)] + [\delta + \epsilon\cos(\omega t)]\sum_{i=1}^{4} a_{ji}^{n}\phi_i[\sigma_j(t)]\psi_p[\sigma_j(t)] - b\sum_{i=1}^{4} a_{ji}^{n-1}\phi_i[\sigma_j(t)]\psi_p[\sigma_j(t)]\right\} d\sigma_j(t) = 0 \quad p = 1,2 \tag{9}$$

where the following weighting functions were applied:

$$\psi_1[\sigma_j(t)] = 1 \tag{10a}$$

$$\psi_2[\sigma_j(t)] = \frac{\sigma_j}{t_j} - \frac{1}{2} \tag{10b}$$

Coefficients from the first two trial functions represent the velocity and displacement at the beginning of each element. These coefficients can be used to relate the states at the beginning of the current period to the states at the end of previous period by

$$\begin{pmatrix} a_{11} \\ a_{12} \end{pmatrix}^n = \begin{pmatrix} a_{E3} \\ a_{E4} \end{pmatrix}^{n-1} \tag{11}$$

The continuity condition of Eq. (11) holds true for coefficients at the beginning and end of each element.

Coefficients of the assumed solution can be related to those of the previous period by arranging Eqs. (9) and (11) into a monodromy operator matrix of size $(2E+2)\times(2E+2)$. The expression for two elements can be written as

$$\begin{bmatrix} 1 & 0 & 0 & 0 & 0 & 0 \\ 0 & 1 & 0 & 0 & 0 & 0 \\ N_{11}^1 & N_{12}^1 & N_{13}^1 & N_{14}^1 & 0 & 0 \\ N_{21}^1 & N_{22}^1 & N_{23}^1 & N_{24}^1 & 0 & 0 \\ 0 & 0 & N_{11}^2 & N_{12}^2 & N_{13}^2 & N_{14}^2 \\ 0 & 0 & N_{21}^2 & N_{22}^2 & N_{23}^2 & N_{24}^2 \end{bmatrix}\begin{bmatrix} a_{11} \\ a_{12} \\ a_{21} \\ a_{22} \\ a_{23} \\ a_{24} \end{bmatrix}^n = \begin{bmatrix} 0 & 0 & 0 & 0 & 1 & 0 \\ 0 & 0 & 0 & 0 & 0 & 1 \\ P_{11}^1 & P_{12}^1 & P_{13}^1 & P_{14}^1 & 0 & 0 \\ P_{21}^1 & P_{22}^1 & P_{23}^1 & P_{24}^1 & 0 & 0 \\ 0 & 0 & P_{11}^2 & P_{12}^2 & P_{13}^2 & P_{14}^2 \\ 0 & 0 & P_{21}^2 & P_{22}^2 & P_{23}^2 & P_{24}^2 \end{bmatrix}\begin{bmatrix} a_{11} \\ a_{12} \\ a_{21} \\ a_{22} \\ a_{23} \\ a_{24} \end{bmatrix}^{n-1} \tag{12}$$

where

$$N_{pi}^j = \int_0^{t_j}\{\ddot{\phi}_i(\sigma_j) + \kappa\dot{\phi}_i(\sigma_j) + [\delta + \epsilon\cos(\omega t)]\phi_i[\sigma_j(t)]\}\psi_p[\sigma_j(t)]d\sigma_j(t) \tag{13}$$

$$P_{pi}^j = b\int_0^{t_j}\phi_i[\sigma_j(t)]\psi_p[\sigma_j(t)]d\sigma_j(t) \tag{14}$$

Equation (12) takes the form of a discrete linear map that can be written as

$$\mathbf{A}\vec{a}_n = \mathbf{B}\vec{a}_{n-1} \quad \text{or} \quad \vec{a}_n = \mathbf{Q}\vec{a}_{n-1} \tag{15}$$

where $\mathbf{Q}=\mathbf{A}^{-1}\mathbf{B}$ is the monodromy operator. The coefficients of the assumed solution, which have been written in vector form $\vec{a}_n$, represent the velocity and displacement at discrete points in time. This provides a dynamic map over a single time delay.

4.1 Map Stability From Characteristic Multipliers. Characteristic multipliers of the transition matrix **Q** determine the stability of the governing equation based on whether they reside within the unit circle (see Sec. 3). The system is stable for a given set of parameters $(\delta, \epsilon, \omega, b)$ if all the characteristic multipliers have modulus <1. In Fig. 1(*a*), a solid line represents the stability boundary ($|\mu|=1$) for a given parameter combination of δ and ϵ. The period of Eq. (1) is 2π, $\kappa=0.1$, and $b=0.01$. The stable region has eigenvalues with a magnitude of <1, and the region marked unstable has eigenvalues with a magnitude >1. Varying ϵ from 0–1 while keeping δ at a constant value of 1.04 provides a transcritical bifurcation (see Fig. 1(*b*)). A flip bifurcation is observed when ϵ is held at a constant of 1 and while δ is varied from 0.4–0.7 (see Fig. 1(*c*)).

5 Single-Element Dynamic Map (*p-Version*)

Although the *h-version* approach can obtain convergence by simply increasing the number of elements, a dramatic increase in computational time often experienced for a larger number of elements (i.e., additional computations are required for the increased matrix size). Therefore, the approach described in Sec. 4 was augmented by increasing the order of approximating polynomials while using a single element. The revised approximate solution becomes

$$x(t) \approx \sum_{i=1}^{s} a_i^n\phi_i[\sigma(t)] \tag{16}$$

where s is the total number of higher-order interpolated polynomials $\phi_i[\sigma(t)]$. The interpolating polynomials, described in Sec. 5.2, are of order p, where

$$p = s - 1 \tag{17}$$

Substitution of the approximate solution (Eq. (16)), into Eq. (1) leads to a nonzero error $e_{rr}(t)$

$$\sum_{i=1}^{s} a_i^n\ddot{\phi}_i[\sigma(t)] + \kappa\sum_{i=1}^{s} a_i^n\dot{\phi}_i[\sigma(t)] + [\delta + \epsilon\cos(\omega t)]\sum_{i=1}^{s} a_i^n\phi_i[\sigma(t)] - b\sum_{i=1}^{s} a_i^{n-1}\phi_i[\sigma(t)] = e_{rr}(t) \tag{18}$$

As in the *h-version*, the integral of weighted error is set to zero; however, this now provides s equations linear in the coefficients of the assumed solution since the weighting functions $\{\psi_i[\sigma(t)]\}$ were chosen to be the same as interpolated polynomials

$$\psi_i[\sigma(t)] = \phi_i[\sigma(t)] \tag{19}$$

$i=1,2,\ldots,s$. This type of integral formulation is known as a weighted Galerkin method [51]. The resultant equation can be written as

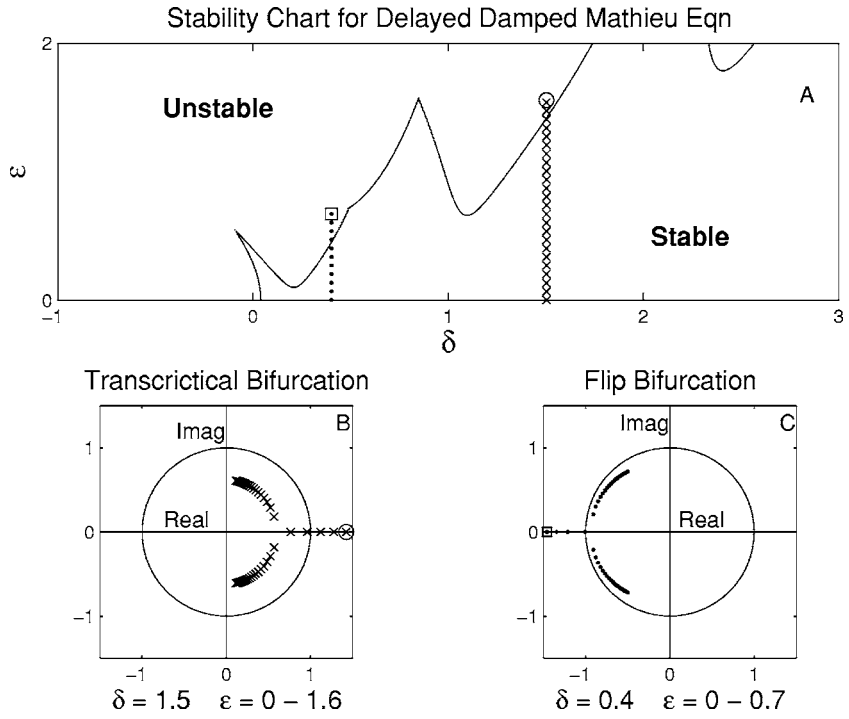

Fig. 1 Multiple element stability predictions (graph A) from characteristic multiplier (μ) trajectories in the complex plane (shown by graphs B and C). The following parameters were used to generate these graphics ω=1, τ=2π, κ=0.1, and b =0.04.

$$\int_0^{t_j}\left\{\sum_{i=1}^{s} a_i^n \ddot{\phi}_i[\sigma(t)]\psi_i[\sigma(t)] + \kappa\sum_{i=1}^{s} a_i^n \dot{\phi}_i[\sigma(t)]\psi_i[\sigma(t)] + [\delta+\epsilon\cos(\omega t)]\sum_{i=1}^{s} a_i^n \phi_i[\sigma(t)]\psi_i[\sigma(t)] - b\sum_{i=1}^{s} a_i^{n-1}\phi_i[\sigma(t)]\psi_i[\sigma(t)]\right\} d[\sigma_j(t)] = 0 \tag{20}$$

where t_j, the integration time for the single element, is equal to the minimal time period T.

The coefficients from the first two trial functions on the first element represent the velocity and displacement at the start of each period. They can be related to the states at the end of the previous period by

$$\begin{pmatrix} a_1 \\ a_2 \end{pmatrix}^n = \begin{pmatrix} a_{s-1} \\ a_s \end{pmatrix}^{n-1} \tag{21}$$

Since initial and final states of the system can be specified in terms of a single polynomial coefficient, a simplistic mapping to the next period can be written with the unity matrix and the identity matrix.

The coefficients of the assumed solution can be related to those of the previous period by arranging Eqs. (20) and (21) into a monodromy operator matrix of size $s \times s$. The expression can be written as

$$\begin{bmatrix} 1 & 0 & 0 & \cdots & 0 & 0 \\ 0 & 1 & 0 & \cdots & 0 & 0 \\ N_{11} & N_{12} & N_{13} & \cdots & N_{1s-1} & N_{1s} \\ N_{21} & N_{22} & N_{22} & \cdots & N_{2s-1} & N_{2s} \\ \vdots & \vdots & \vdots & \ddots & \vdots & \vdots \\ N_{s1} & N_{s2} & N_{s3} & \cdots & N_{ss-1} & N_{ss} \end{bmatrix} \begin{bmatrix} a_1 \\ a_2 \\ a_3 \\ a_4 \\ \vdots \\ a_s \end{bmatrix}^n = \begin{bmatrix} 0 & 0 & 0 & \cdots & 1 & 0 \\ 0 & 0 & 0 & \cdots & 0 & 1 \\ P_{11} & P_{12} & P_{13} & \cdots & P_{1s-1} & P_{1s} \\ P_{21} & P_{22} & P_{22} & \cdots & P_{2s-1} & P_{2s} \\ \vdots & \vdots & \vdots & \ddots & \vdots & \vdots \\ P_{s1} & P_{s2} & P_{s3} & \cdots & P_{ss-1} & P_{ss} \end{bmatrix} \begin{bmatrix} a_1 \\ a_2 \\ a_3 \\ a_4 \\ \vdots \\ a_s \end{bmatrix}^{n-1} \tag{22}$$

where

$$N_{ii} = \int_0^{t_j} \{\ddot{\phi}_i[\sigma(t)] + \kappa\dot{\phi}_i[\sigma(t)] + [\delta+\epsilon\cos(\omega t)]\phi_i[\sigma(t)]\}\psi_i[\sigma(t)]d\sigma(t) \tag{23}$$

$$P_{ii} = b\int_0^{t_j} \phi_i[\sigma(t)]\psi_i[\sigma(t)]d\sigma(t) \tag{24}$$

A discrete linear map, described by Eq. (22), can be written as

$$\mathbf{A}\vec{a}_n = \mathbf{B}\vec{a}_{n-1} \quad \text{or} \quad \vec{a}_n = \mathbf{Q}\vec{a}_{n-1} \tag{25}$$

where the monodromy operator $\mathbf{Q}$ can be found from the pseudo-inverse $\mathbf{Q}=[(\mathbf{A}^T\mathbf{A})^{-1}\mathbf{A}^T]\mathbf{B}$. Alternatively, although this problem

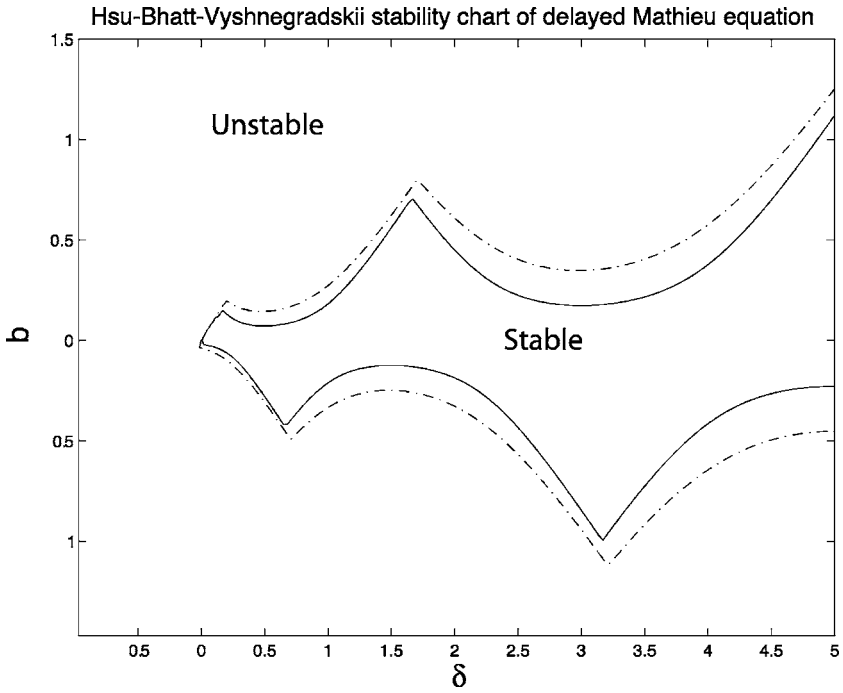

Fig. 2 Delayed Mathieu equation stability chart for two damping coefficient values: solid line indicates κ=0.1; dotted line indicates κ=0.2. The other parameters used to generate this graph are ω=1, τ=2π, and ϵ=0.

was not experienced for the system under study, the matrix pseudo inverse could result in numerical difficulties and other methods of matrix decomposition may be necessary.

5.1 Stability. As discussed in Sec. 4.1, the condition for asymptotic stability (see Figs. 2 and 3) is that the characteristic multipliers (μ_i) of the transition matrix **Q** should satisfy the following condition:

$$\max|\mu_i| < 1 \tag{26}$$

where $i=1,2,\ldots s$. Figure 2 represents the stability boundaries ($|\mu|=1$) of delayed Mathieu equation for different values of κ. The region enclosed by stability boundary for a given κ is stable ($|\mu|<1$) and vice versa. In both cases ϵ=0, period equals time delay $\tau = 2\pi$, and convergence was obtained using seventh order polynomials. Figure 3 is a three-dimensional graphical representation of stablility in (b,δ,ϵ) parameter space. The region enclosed within the surface is stable, and the surface ($|\mu|=1$) represents the transition from stable to unstable region. Here κ=0.2, time delay τ=2π, and ω=1.

5.2 Interpolated Polynomials. For convergence of a second-order differential system, the trial functions or interpolated polynomials, must satisfy at least two conditions: C^0 continuity and a complete polynomial of the first degree [53]. Completeness is ensured by increasing the degree of the polynomials while preserving C^0 continuity. The *single-element* approach requires an element that exceeds a minimal C^0 continuity condition (i.e., an element with C^1 continuity to obtain better convergence). To derive the polynomials with C^1 continuity, each polynomial and its derivatives were interpolated at interelement nodes. This requires two boundary conditions at each interelement node.

The interpolated polynomials obey the following relationships on the local time interval of $0 \geq \sigma/t_j \geq 1$:

$$\sum_{i=1}^{s} \phi_i[\sigma(t)] = 1 \tag{27a}$$

$$\sum_{i=1}^{s} \dot{\phi}_i[\sigma(t)] = 1 \tag{27b}$$

where ϕ is an interpolated polynomial. Polynomials are of order (p), which is related to the total number of polynomials by $p=s-1$. Cubic Hermite polynomials, Eq. (7), represent a set of the lowest-degree polynomials with C^1 continuity. As an example, the expressions for a set of fifth order interpolating polynomials are given in the Appendix.

Figures 4(a) and 4(b) represent the displacement and velocity constraints in local time, respectively, for fifth-order interpolated polynomials (p=5,s=6). The local time is divided into three nodes, which include two boundary nodes and one intermittent node. The sum of displacement and velocity at each node is 1. Constraining interpolated polynomials in this fashion helps maintain completeness, C^1 continuity, and orthogonality.

6 Monodromy Operator Period

The delayed damped Mathieu equation is a second-order differential equation with a periodic coefficient and a time-delay term proportional to b. The coefficient $\delta+\epsilon\cos(\omega t)$ is the aforementioned time-periodic function with a period of $T_p=2\pi/\omega$ and τ provides the constant time delay. In the stability investigations of the previous sections, the time delay has been set equal to the period of the time-periodic coefficient. When considering the correct time interval for computing the monodromy operator, this gives rise to an interesting question. For instance, should the Floquet matrix, or monodromy operator **Q**, be computed over the period of the time delay or over a period of the time-periodic coefficient? Therefore, the following three cases are noteworthy: (i) the time delay is equal to the periodic coefficient period $\tau=T_p$; (ii) the time delay is less than the periodic coefficient period $\tau<T_p$; and (iii) the time delay is greater than the periodic coefficient period $\tau>T_p$.

Since the case of the equivalent periods, $\tau=T_p$, has already been discussed, the remaining question is how to handle the last

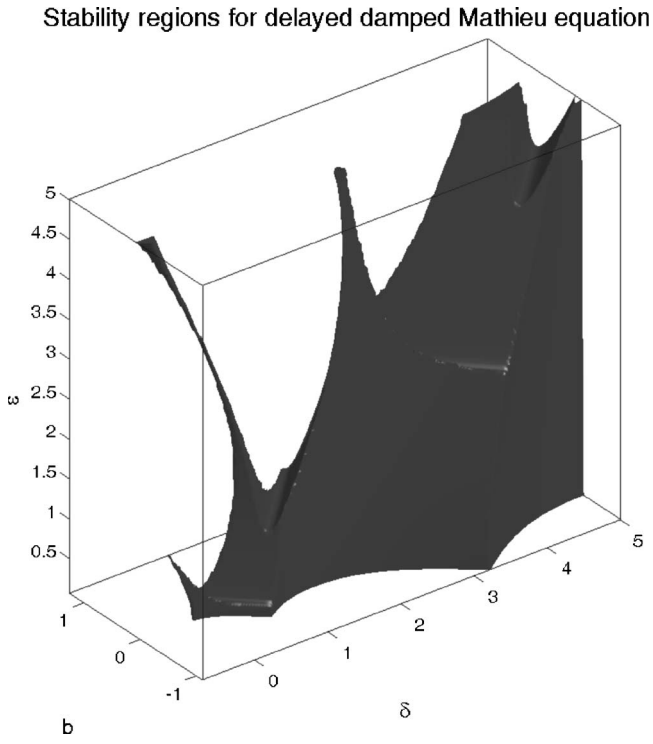

Fig. 3 Three-dimensional plot depicting stability regions for the DDME with respect to parameters δ, b, and ϵ. Shaded regions are stable, and unstable regions are transparent. Predictions are for $\kappa=0.2$, $\tau=2\pi$, and $\omega=1$.

two cases. Therefore, the case of $\tau > T_p$ is examined in Fig. 5 by computing the monodromy operator over the delay period $\tau=2\pi$ and the periodic coefficient period $T_p=2$. When numerical simulation is used to study points of disagreement, the results show the stability boundaries computed for a period of $T=2$ are correct. However, based solely on this result, one cannot conclude whether using the minimal period or always using the periodic coefficient period, $T_p=2\pi/\omega$, is correct. The answer to this question is clarified by examining the case of $\tau < T_p$ (see Fig. 6). When numerical simulation is used to study points of disagreement, it is found that the correct stability boundaries are obtained when the monodromy operator is computed over a period of $T=4\pi$. This reveals that the Floquet matrix should be computed over the periodic coefficient period. This conclusion is in direct agreement with the results presented by Insperger and Stépán [52].

7 Damped Mathieu Equation (DME)

This section considers a special case of the DDME, the damped Mathieu equation, which is obtained by setting $b=0$ in the previous studies. Here, a single-element monodromy operator is formed from the application of higher-order polynomials. The equation of interest is

$$\ddot{x}(t) + \kappa\dot{x}(t) + [\delta + \epsilon\cos(\omega t)]x(t) = 0 \tag{28}$$

Substitution of the assumed solution, Eq. (16), into Eq. (28), leads to a nonzero error $e_{rr}(t)$

$$\sum_{i=1}^{s} a_i^n \ddot{\phi}_i[\sigma(t)] + \kappa\sum_{i=1}^{s} a_i^n \dot{\phi}_i[\sigma(t)] + [\delta + \epsilon\cos(\omega t)]\sum_{i=1}^{s} a_i^n \phi_i[\sigma(t)] = e_{rr}(t) \tag{29}$$

Applying the Galerkin residual method (see Sec. 5), we have

$$\int_0^{t_j} \left\{ \sum_{i=1}^{s} a_i^n \ddot{\phi}_i[\sigma(t)]\psi_i[\sigma(t)] + \kappa\sum_{i=1}^{s} a_i^n \dot{\phi}_i[\sigma(t)]\psi_i[\sigma(t)] + [\delta + \epsilon\cos(\omega t)]\sum_{i=1}^{s} a_i^n \phi_i[\sigma(t)]\psi_i[\sigma(t)] \right\} d[\sigma(t)] = 0 \tag{30}$$

Once again, the continuity condition, given in Eq. (21), is implied to relate the coefficients at the beginning and end of each period.

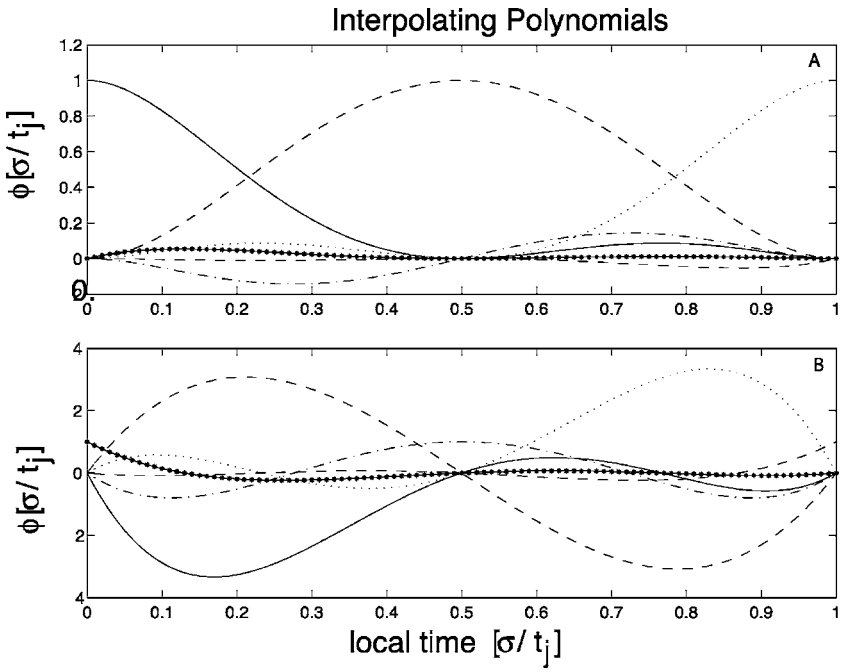

Fig. 4 Fifth-order interpolated polynomials plotted as a function of the normalized local time

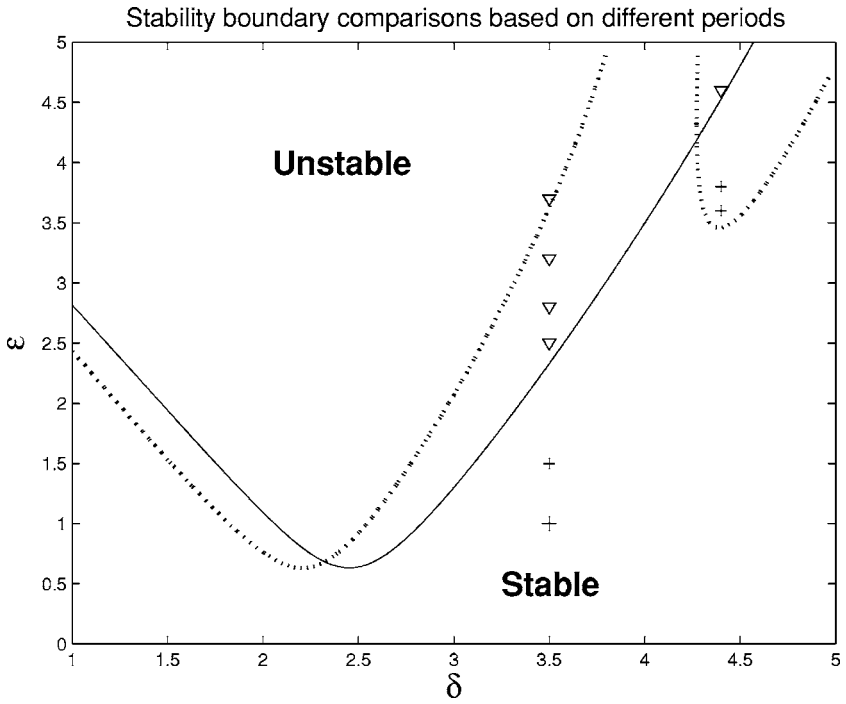

Fig. 5 Stability boundaries are computed when evaluating the Floquet matrix over a period of 2π (dotted line) and a period of 2 (solid line). Stable simulated results are shown by +, and unstable simulation results are shown by ▽. Other parameters used for the computations are κ=0.2, b=0.01, $\tau=2\pi$, and $\omega=\pi$.

The monodromy operator for the damped Mathieu equation, Eq. (28), results in a special case of Eq. (22), where $P_{ii}=0$. Applying the discretization approach of Sec. 6, one develops the following matrix equation:

$$\begin{bmatrix} 1 & 0 & 0 & \dots & 0 & 0 \\ 0 & 1 & 0 & \dots & 0 & 0 \\ N_{11} & N_{12} & N_{13} & \dots & N_{1s-1} & N_{1s} \\ N_{21} & N_{22} & N_{22} & \dots & N_{2s-1} & N_{2s} \\ \vdots & \vdots & \vdots & \ddots & \vdots & \vdots \\ N_{s1} & N_{s2} & N_{s3} & \dots & N_{ss-1} & N_{ss} \end{bmatrix} \begin{bmatrix} a_1 \\ a_2 \\ a_3 \\ a_4 \\ \vdots \\ a_s \end{bmatrix}^n$$

$$= \begin{bmatrix} 0 & 0 & 0 & \dots & 1 & 0 \\ 0 & 0 & 0 & \dots & 0 & 1 \\ 0 & 0 & 0 & \dots & 0 & 0 \\ 0 & 0 & 0 & \dots & 0 & 0 \\ \vdots & \vdots & \vdots & \ddots & \vdots & \vdots \\ 0 & 0 & 0 & \dots & 0 & 0 \end{bmatrix} \begin{bmatrix} a_1 \\ a_2 \\ a_3 \\ a_4 \\ \vdots \\ a_s \end{bmatrix}^{n-1} \tag{31}$$

where N_{ii} is given by Eq. (23).

A discrete linear map, described by Eq. (31), can be written as

$$\mathbf{A}\vec{a}_n = \mathbf{B}\vec{a}_{n-1} \tag{32}$$

where $\mathbf{Q}=[(\mathbf{A}^T\mathbf{A})^{-1}\mathbf{A}^T]\mathbf{B}$. For stability, all characteristic multipliers of the transition matrix ($\mathbf{Q}$) should have magnitude of <1 for a given combination of δ, ω, ϵ. In Fig. 7, a solid line indicates the stability boundary of damped Mathieu Eq. (28) for κ=0.1 and dotted line for κ=0.2. The period of Eq. (28) is 2π, and convergence was obtained using ninth-order polynomials.

7.1 Floquet Transition Matrix. As one might expect, the Floquet transition matrix for the DME should be related to Eq. (31). To illustrate this, the pseudo inverse of Eq. (31) is taken to arrive at the following revised equation form:

$$\begin{bmatrix} a_1 \\ a_2 \\ \vdots \\ a_{s-1} \\ a_s \end{bmatrix}^n = \begin{bmatrix} 0 & 0 & \dots & 0 & c_1 & c_2 \\ 0 & 0 & \dots & 0 & c_3 & c_4 \\ \vdots & \vdots & \ddots & \vdots & \vdots & \vdots \\ 0 & 0 & \dots & 0 & \varphi_{11} & \varphi_{12} \\ 0 & 0 & \dots & 0 & \varphi_{21} & \varphi_{22} \end{bmatrix} \begin{bmatrix} a_1 \\ a_2 \\ \vdots \\ a_{s-1} \\ a_s \end{bmatrix}^{n-1} \tag{33}$$

where $c_i\,(i=1,2,3,\dots)$ are constant terms in $\mathbf{Q}$, $a_1,a_2,\dots,a_{s-1},a_s$ are the coefficients of the assumed solution, which happen to represent the velocity and displacement at specific local times, and n represents the period. The terms φ_{11}, φ_{12}, φ_{21}, and φ_{22} are the elements of the Floquet transition matrix (φ). Therefore, from Eq. (33), we have

$$\varphi = \begin{bmatrix} \varphi_{11} & \varphi_{12} \\ \varphi_{21} & \varphi_{22} \end{bmatrix} \tag{34}$$

Once the Floquet transition matrix is found, stability is determined from the eigenvalues of this matrix (see Sec. 3 for details).

8 Error Analysis

The error analysis accounts for the discretization error and assumes all other forms of error are absent. Discretization error is caused by using a finite number of trial functions $\phi[\sigma(t)]$ and a discrete set of coefficients a_i in the assumed solution to approximate the exact solution for $x[\sigma(t)]$.

The completeness and continuity are two minimum conditions required to closely approximate the second-order system with a linear combination of trial functions. The measured energy error provides a metric for closeness, where

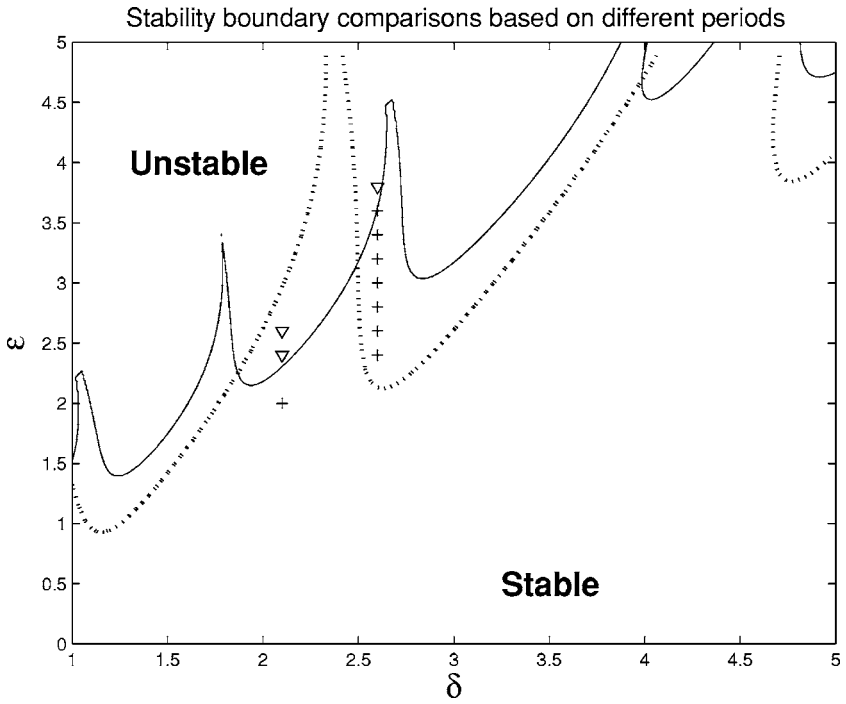

Fig. 6 Stability boundaries are computed when evaluating the Floquet matrix over $T=2\pi$ (dotted line) and $T=4\pi$ (solid line). Stable simulated results are shown by + and unstable simulation results are shown by ▽. Other parameters used for the computations are $\kappa=0.2$, $b=0.01$, $\tau=2\pi$, and $\omega=1/2$.

$$\text{Energy Error} = \left(\int_{\text{domain}} E[\sigma(t)]D\{E[\sigma(t)]\}dt \right)^{1/2} \tag{35}$$

and

$$E[\sigma(t)] = x[\sigma(t)] - \sum_{i=1}^{s} a_i^n \phi_i[\sigma(t)] \tag{36}$$

and D is the differential operator for the governing differential equation (1). In physical applications, the expression $E[\sigma(t)]D\{E[\sigma(t)]\}$, or similarly $x[\sigma(t)]D\{x[\sigma(t)]\}$, generally correspond to energy density. The polynomial solutions will converge as p approaches infinity [53].

It can be shown that the eigenvalues converge at the same rate as the global energy, (i.e., the rate of convergence of global energy is of the order of $O(E^{2(p-m+1)})$, where $2m$ is the order of governing differential equation, p is the polynomial order, and E is the number of time elements). This is because in physical systems, the eigenvalue is either the global energy or the ratio of global potential energy to global kinetic energy [53].

Extrapolation is one of the most common methods to estimate convergence [51]. The assumption underlying this method is that a solution is always available at each refinement step.

This paper discusses two different approaches to extrapolate convergence.

Two-point extrapolation. As already discussed, eigenvalues have the same rate of convergence as global energy [53]. Therefore convergence of an approximated eigenvalue to exact eigenvalue is one criterion for minimization of error. The exponential extrapolation can be written as

$$\mu_{\text{est}} = \mu_{\text{ext}}(1 - e^{ap}) \tag{37}$$

where μ_{est} is an extrapolated eigenvalue, a is an unknown constant, and p is the polynomial order. Initially, to solve for a, μ_{est} is the eigenvalue corresponding to the maximum eigenvalue gradient at a low polynomial order. Figure 8 represents a particular case of delayed Mathieu equation (1) where $\kappa=0.2$, period is 2π and $\omega=1$. Third-order interpolated polynomials are used to predict $\mu \approx 15.83$ corresponding to the maximum gradient. Therefore, in a two-point extrapolation, $\mu_{\text{est}}=15.83$. The corresponding exact eigenvalue μ_{ext} is found using Euler time marching (simulation). The system was simulated using the same values of parameters (δ, ϵ, b) corresponding to maximum eigenvalue gradient, and the Floquet transition matrix (φ) was computed looking back one time period. The maximum eigenvalue of φ is (μ_{ext}).

$$\mu_{\text{ext}} = \max|(\mu I - \varphi) = 0| \tag{38}$$

Three-point extrapolation. This approach [51,54] requires a three-element solution corresponding to polynomial order p, $p-1$, and $p-2$. The exact solution of $\|x(t)\|^2$ can be estimated by solving

$$\frac{\|x(t)\|^2 - \|x(t)_p\|^2}{\|x(t)\|^2 - \|x(t)_{p-1}\|^2} = \left(\frac{\|x(t)\|^2 - \|x(t)_{p-1}\|^2}{\|x(t)\|^2 - \|x(t)_{p-2}\|^2} \right)^{\log(p-1/p)/\log(p-2/p-1)} \tag{39}$$

where $\|x(t)\|^2$ represents the energy form of $x(t)$ and p is the polynomial order. Considering eigenvalues (μ) have the same rate of convergence as global energy, Eq. (39) can be rewritten as

$$\frac{\mu^2 - \mu_p^2}{\mu^2 - \mu_{p-1}^2} = \left(\frac{\mu^2 - \mu_{p-1}^2}{\mu^2 - \mu_{p-2}^2} \right)^{\log(p-1/p)/\log(p-2/p-1)} \tag{40}$$

where μ is the exact eigenvalue calculated from a time-marching algorithm. Once μ is known μ_p can be calculated using (40).

Both two- and three-point extrapolation techniques were found to have close agreement with the predicted eigenvalues. In Fig. 9, dots represent the three-point extrapolation technique and the dotted line with circles indicates the two-point extrapolation whereas the solid line depicts the true eigenvalue as computed from Euler

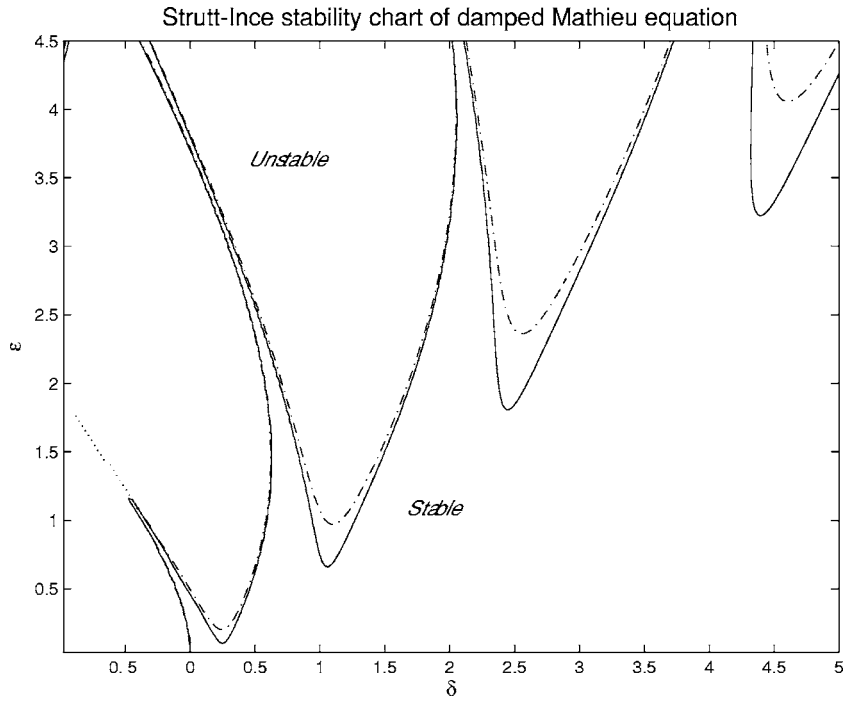

Fig. 7 Stability boundaries of damped Mathieu equation. Predictions are for κ =0.1 (solid line) and κ=0.2 (dotted line).

simulation. Although complete convergence to the true solution is possible only when p approaches infinity, an optimum value of p is selected based on an error tolerance.

9 Summary and Conclusions

This paper investigates the effect of a single time delay and a periodic coefficient on the stability of the delayed damped Mathieu equation. Stability behavior is investigated using two different techniques: a single-element (*p-version*) time finite element method; and a multiple-element (*h-version*) temporal finite element method. In both cases, the exact solution is approximated with a set of interpolated polynomials. The stability of the system is determined by the characteristic multipliers of the discrete linear map. The latter approach uses only one temporal element, but obtains convergence with a set of higher-order orthogonal polynomials. On the other hand, the *h*-version uses cubic polynomials

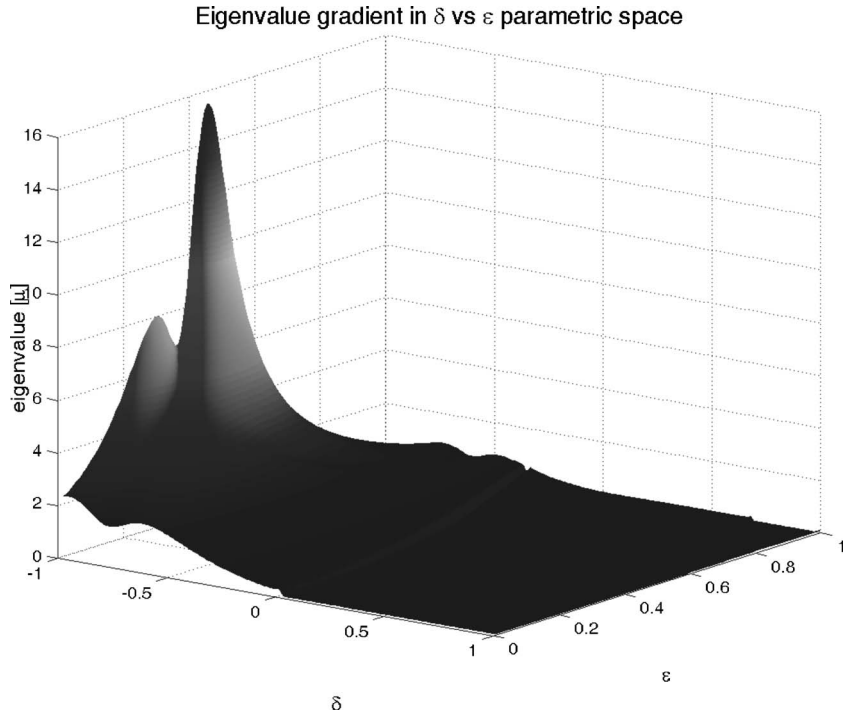

Fig. 8 Gradient plot of eigenvalues (μ) in δ versus ϵ parameter space

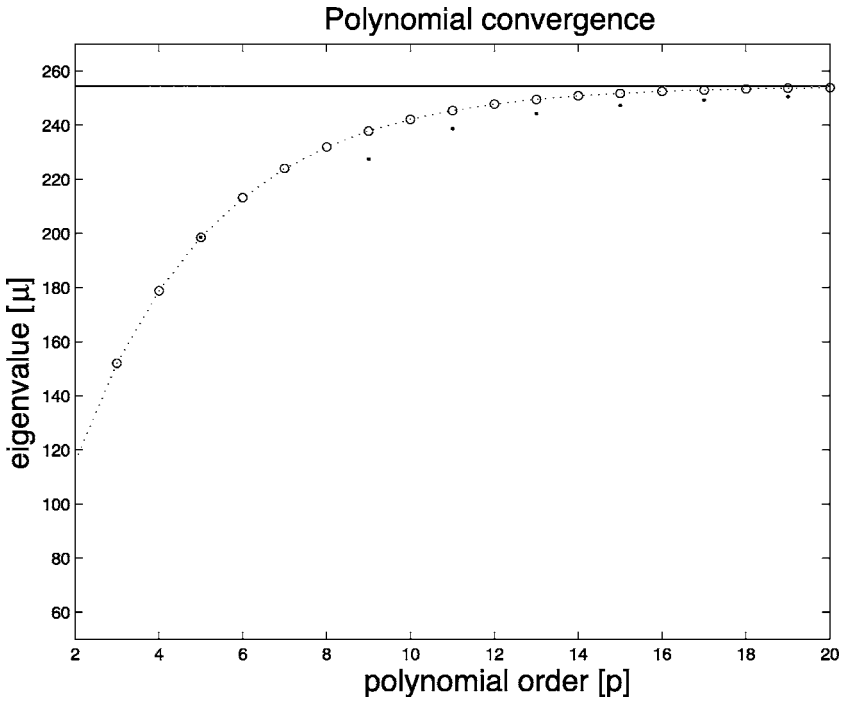

Fig. 9 Convergence of eigenvalue (μ) to true eigenvalue with an increase in polynomial order

and an increasing number of elements to ensure convergence. The rate of convergence of the *p*-version was found to be very quick—a more rapid convergence is obtained when *p* is increased as compared to increasing the number of elements in *h*-version. However, due to symbolic manipulation, the *p*-version becomes more complicated and computationally expensive as the polynomial order is increased beyond a certain value. Results obtained from both approaches were verified using time domain simulation. The developed temporal finite element approach is shown to be a powerful and flexible approach to the solution of equations with a periodic coefficient and a single time delay.

In planned future work, both *p*- and *h*-versions can be combined to form a more versatile *hp*-version of the temporal finite element method for delay equations.

Acknowledgment

Support from U.S. National Science Foundation CAREER Award (CMS-0348288) is gratefully acknowledged.

Appendix

$$\phi_1(\sigma) = 1 - 23\left(\frac{\sigma(t)}{t_j}\right)^2 + 66\left(\frac{\sigma(t)}{t_j}\right)^3 - 68\left(\frac{\sigma(t)}{t_j}\right)^4 + 24\left(\frac{\sigma(t)}{t_j}\right)^5 \tag{41a}$$

$$\phi_2(\sigma) = t_j\left[\left(\frac{\sigma(t)}{t_j}\right) - 6\left(\frac{\sigma(t)}{t_j}\right)^2 + 13\left(\frac{\sigma(t)}{t_j}\right)^3 - 12\left(\frac{\sigma(t)}{t_j}\right)^4 + 4\left(\frac{\sigma(t)}{t_j}\right)^5\right] \tag{41b}$$

$$\phi_3(\sigma) = 16\left(\frac{\sigma(t)}{t_j}\right)^2 - 32\left(\frac{\sigma(t)}{t_j}\right)^3 + 16\left(\frac{\sigma(t)}{t_j}\right)^4 \tag{41c}$$

$$\phi_4(\sigma) = t_j\left[-8\left(\frac{\sigma(t)}{t_j}\right)^2 + 32\left(\frac{\sigma(t)}{t_j}\right)^3 - 40\left(\frac{\sigma(t)}{t_j}\right)^4 + 16\left(\frac{\sigma(t)}{t_j}\right)^5\right] \tag{41d}$$

$$\phi_5(\sigma) = 7\left(\frac{\sigma(t)}{t_j}\right)^2 - 34\left(\frac{\sigma(t)}{t_j}\right)^3 + 52\left(\frac{\sigma(t)}{t_j}\right)^4 - 24\left(\frac{\sigma(t)}{t_j}\right)^5 \tag{41e}$$

$$\phi_6(\sigma) = t_j\left[-\left(\frac{\sigma(t)}{t_j}\right)^2 + 5\left(\frac{\sigma(t)}{t_j}\right)^3 - 8\left(\frac{\sigma(t)}{t_j}\right)^4 + 4\left(\frac{\sigma(t)}{t_j}\right)^5\right] \tag{41f}$$

References

[1] Insperger, T., Mann, B. P., Stépán, G., and Bayly, P. V., 2003, "Stability of Up-Milling and Down-Milling, Part 1. Alternative Analytal Methods," Int. J. Mach. Tools Manuf., **43**, pp. 25–34.
[2] Mann, B. P., Insperger, T., Bayly, P. V., and Stépán, G., 2003, "Stability of Up-Milling and Down-Milling, Part 2: Experimental Verification," Int. J. Mach. Tools Manuf., **43**, pp. 35–40.
[3] Altintas, Y., and Budak, E., 1995, "Analytical Prediction of Stability Lobes in Milling," CIRP Ann., **44**(1), pp. 357–362.
[4] Mann, B. P., Garg, N. K., Young, K. A., and Helvey, A. M., 2005, "Milling Bifurcations From Structural Asymmetry and Nonlinear Regeneration," Nonlinear Dyn., **42**(4), Dec, pp. 319–337.
[5] Balachandran, B., 2001, "Nonlinear Dynamics of Milling Process," Proc. R. Soc. London, Ser. A, **359**, pp. 793–819.
[6] Yang, B., and Wu, X., 1998, "Modal Expansion of Structural Systems With Time Delays," AIAA J., **36**(12), pp. 2218–2224.
[7] Yakubovitch, V. A., and Starzhinskii, V. M., 1975, *Linear Differential Equations With Periodic Coefficients*, Wiley, New York.
[8] Lindh, K. G., and Likins, P. W., 1970, "Infinite Determinant Methods for Stability Analysis of Periodic-Coefficient Differential Equations," AIAA J., **8**, pp. 680–686.

[9] Brockett, R. W., 1970, *Finite Dimensional Linear Systems*, John Wiley, New York.
[10] Peters, D. A., and Hohenemser, K. H., 1971, "Application of Floquet Transition Matrix to Problems of Lifting Rotor Stability," J. Am. Helicopter Soc., **16**, pp. 25–33.
[11] Hsu, C. S., and Cheng, W. H., 1973, "Application of the Theory of Impulsive Parametric Excitation and New Treatment of General Parametric Excitation Problems," ASME J. Appl. Mech., **40**, pp. 78–86.
[12] Hsu, C. S., 1974, "On Approximating a General Linear Periodic System," J. Math. Anal. Appl., **45**, pp. 234–251.
[13] Sinha, S. C., Chou, C. C., and Denman, H. H., 1979, "Stability Analysis of Systems With Periodic Coefficients: An Approximate Approach," J. Sound Vib., **64**, pp. 515–527.
[14] Friedmann, P., Hammond, C. C., and Woo, T. H., 1977, "Efficient Numerical Treatment of Periodic Systems With Applications to Stability Problems," Int. J. Numer. Methods Eng., **11**, pp. 1117–1136.
[15] Gockel, M. A., 1972, "Practical Solution of Linear Equations With Periodic Coefficients," J. Am. Helicopter Soc., **17**, pp. 2–10.
[16] Gaonkar, G. H., Prasad, D. S. S., and Sastry, D., 1981, "On Computing Floquet Transition Matrices of Rotocraft," J. Am. Helicopter Soc., **26**, pp. 56–61.
[17] Nayfeh, A. H., 1973, *Perturbation Methods*, Wiley, New York.
[18] Jordan, D. W., and Smith, P., 1977, *Nonlinear Ordinary Differential Equations*, Clarendon Press, Oxford.
[19] Sinha, S. C., and Wu, D. H., 1991, "An Efficient Computational Scheme for Analysis of Periodic Systems," J. Sound Vib., **151**(1), pp. 91–117.
[20] Sinha, S. C., 1997, "On the Analysis of Time-Periodic Nonlinear Dynamical Systems," Sadhana: Proc., Indian Acad. Sci., **22**(3), pp. 411–434.
[21] Sinha, S. C., Pandiyan, R., and Bibb, J. S., 1996, "Liapunov-Floquet Transformation: Computation and Applications to Periodic Systems," ASME J. Vibr. Acoust., **118**, pp. 209–219.
[22] Sinha, S. C., Wu, D. H., Juneja, V., and Joseph, P., 1991, "An Approximate Analytical Solution for Systems With Periodic Coefficients via Symbolic Computation," AIAA/ASME/ASCE/AHS/ASC 32nd Structures, Structural Dynamics and Materials Conference, April, pp. 790–797.
[23] Joseph, P., Pandiyan, R., and Sinha, S. C., 1993, "Optimal Control of Mechanical Systems Subjected to Periodic Loading via Chebyshev Polynomials," Opt. Control Appl. Methods, **14**, pp. 75–90.
[24] Butcher, E. L., Ma, H., Bueler, E., Averina, V., and Szabo, Z., 2004, "Stability of Linear Time-Periodic Delay-Differential Equations via Chebyshev Polynomials," Int. J. Numer. Methods Eng., **59**(7), pp. 895–922.
[25] Ma, H., Deshmukh, V., Butcher, E. A., and Averina, V., 2005, "Delayed State Feedback and Chaos Control for Time-Periodic Systems via a Symbolic Approach," Commun. Nonlinear Sci. Numer. Simul., **10**, pp. 467–580.
[26] Ma, H., Butcher, E. A., and Bueler, E., 2003, "Chebyshev Expansion of Linear and Peicewise Linear Dynamic Systems With Time Delay and Periodic Coefficients Under Control Excitations," ASME J. Dyn. Syst., Meas., Control, **125**, pp. 236–243.
[27] Bueler, E., Averina, V., and Butcher, E. A., 2004, "Periodic Linear DDEs: Collocation Approximation to the Monodromy Operator," SIAM Annual Meeting, Portland, Oregon.
[28] Szabo, S., and Butcher, E. A., 2002, "Stability Analysis of Delayed 2nd Order Odes Based on the Method of Chebyshev Polynomials," European Conference on Numerical Methods of Computational Mechanics, July 15–19, Miskolc, Hungary.
[29] Horng, I. R., and Chou, J. H., 1985, "Analysis Parameter Estimation and Optimal Control of Time-Delay Systems via Chebyshev Series," Int. J. Control, **41**, pp. 1221–1234.
[30] Chung, H. Y., and Sun, Y. Y., 1987, "Analysis of Time-Delay Systems Using an Alternative Technique," Int. J. Control, **46**, pp. 1621–1631.
[31] Mathieu, E., 1868, "Memoire sur le Mouvement Vibratorie d'une Membrane de Forme Elliptique," J. Math, **13**, pp. 137–203.
[32] Bellman, R., and Cooke, K., 1963, *Differential-Difference Equations*, Academic Press, New York.
[33] Bhatt, S. J., and Hsu, C. S., 1966, "Stability Criteria for Second-Order Dynamical Systems With Time Lag," Appl. Math. (Germany), **33**, pp. 113–118.
[34] Niemark, J., 1949, "D-Subdivision and Spaces of Quasi-Polynomials," Prikl. Mat. Mekh., **13**, pp. 349–380 (in Russian).
[35] Andreev, A. F., 1958, "Twelve Papers on Function Theory, Probability and Differential Equations," American Mathematical Society, Series 2, Volume 8.
[36] Insperger, T., and Stépán, G., 2002, "Stability Chart of the Delayed Mathieu Equation," Proc. R. Soc. London, Ser. A, **458**, pp. 1989–1998.
[37] Insperger, T., and Stépán, G., 2001, "Semi-Discretization of Delayed Dynamical Systems," *Proc. of ASME 2001 Design Engineering Technical Conferences and Computers and Information in Engineering Conference*, Pittsburgh, ASME, New York.
[38] Insperger, T., and Stépán, G., 2002, "Semi-Discretization Method for Delayed Systems," Int. J. Numer. Methods Eng., **55**(5), pp. 503–518.
[39] Chang, P. Y., Yang, S. Y., and Wang, M. L., 1986, "Solution of Linear Dynamic Systems by Generalized Orthogonal Polynomials," Int. J. Syst. Sci., **17**, pp. 1727–1740.
[40] Sinha, S. C., and Chou, C. C., 1976, "An Approximate Analysis of Transient Response of Time Dependent Linear Systems by Orthogonal Polynomials," J. Sound Vib., **49**, pp. 309–326.
[41] Lindlbauer, M., 1998, "On the Rate of Convergence of the Laws of Markov Chains Associated With Orthogonal Polynomials," J. Comput. Appl. Math., **99**, pp. 287–297.
[42] Halley, J. E., 1999, "Stability of Low Radial Immersion Milling," Master's thesis, Washigton University, Saint Louis.
[43] Bayly, P. V., Halley, J. E., Mann, B. P., and Davis, M. A., 2003, "Stability of Interrupted Cutting by Temporal Finite Element Analysis," ASME J. Manuf. Sci. Eng., **125**, pp. 220–225.
[44] Mann, B. P., 2003, "Dynamic Models of Milling and Broaching," Ph.D. dissertation, Washington University, Saint Louis, May.
[45] Mann, B. P., Bayly, P. V., Davies, M. A., and Halley, J. E., 2004, "Limit Cycles, Bifurcations, and the Accuracy of the Milling Process," J. Sound Vib., **277**, pp. 31–48.
[46] Mann, B. P., Young, K. A., Schmitz, T. L., and Dilley, D. N., 2005, "Simultaneous Stability and Surface Location Error Predictions in Milling," ASME J. Manuf. Sci. Eng., **127**, pp. 446–453.
[47] Nayfeh, A. H., and Balachandran, B., 1995, *Applied Non-linear Dynamics Analytical, Computational and Experimental Methods*, Wiley, New York, Wiley Series on Nonlinear Science.
[48] Hale, J. K., and Lunel, S. V., 1993, *Introduction to Functional Differential Equations*, Springer-Verlag, Berlin.
[49] Hassard, B. D., 1997, "Counting Roots of the Characteristic Equation for Linear Delay-Differential Systems," J. Differ. Equations, **136**, pp. 222–235.
[50] Mann, B. P., Garg, N. K., Young, K. A., and Helvey, A. M., 2005, "Milling Bifurcations From Structural Asymmetry and Nonlinear Regeneration," Nonlinear Dyn., **42**(4), pp. 319–337.
[51] Zienkiewicz, O. C., and Taylor, R. L., 2000, *The Finite Element Method*, 5th ed., Butterworth Heinemann, Oxford, Vol. 1.
[52] Insperger, T., and Stépán, G., 2004, "Updated Semi-Discretization Method for Periodic Delay-Differential Equations With Discrete Delay," Int. J. Numer. Methods Eng., **61**, pp. 117–141.
[53] Burnett, D. S., 1988, *Finite Element Analysis (From Concepts to Applications)*, 5th ed., Addison-Wesley, Reading, MA.
[54] Zienkiewicz, O. C., Zhu, J. Z., and Gong, N. G., 1989, "Effective and Practical h-p Version Adaptive Analysis Procedures for the Finite Element Method," Int. J. Numer. Methods Eng., **28**, pp. 879–891.